

Tissue-Specific Cultured Human Pericytes: Perivascular Cells from Smooth Muscle Tissue Have Restricted Mesodermal Differentiation Ability

This is the peer reviewed version of the following article:

Original:

Pierantozzi, E., Vezzani, B., Badin, M., Curina, C., Severi, F.M., Petraglia, F., et al. (2016). Tissue-Specific Cultured Human Pericytes: Perivascular Cells from Smooth Muscle Tissue Have Restricted Mesodermal Differentiation Ability. *STEM CELLS AND DEVELOPMENT*, 25(9), 674-686 [10.1089/scd.2015.0336].

Availability:

This version is available <http://hdl.handle.net/11365/1002026> since 2019-04-29T20:38:06Z

Published:

DOI: <http://doi.org/10.1089/scd.2015.0336>

Terms of use:

Open Access

The terms and conditions for the reuse of this version of the manuscript are specified in the publishing policy. Works made available under a Creative Commons license can be used according to the terms and conditions of said license.

For all terms of use and more information see the publisher's website.

(Article begins on next page)

Tissue-specific cultured human pericytes: perivascular cells from smooth muscle tissue have restricted mesodermal differentiation ability

Enrico Pierantozzi^{a*}, Bianca Vezzani^{a*}, Margherita Badin^a, Carlo Curina^a, Filiberto Maria Severi^b, Felice Petraglia^b, Davide Randazzo^a, Daniela Rossi^a, Vincenzo Sorrentino^a

^aMolecular Medicine Section and ^bDivision of Obstetrics and Gynecology, Department of Molecular and Developmental Medicine, University of Siena, Via Aldo Moro 2, 53100 Siena, Italy. * Enrico Pierantozzi and Bianca Vezzani contributed equally to this article.

Enrico Pierantozzi: e-mail pierantozzi@unisi.it; Phone +39057723-4153; fax -4191

Bianca Vezzani: e-mail bianca.vezzani88@gmail.com; Phone +39057723-4153; fax -4191

Margherita Badin: e-mail marbad.it@gmail.com; Phone +39057723-4153; fax -4191

Carlo Curina: curinac@yahoo.it; Phone +39057723-4153; fax -4191

Filiberto Maria Severi: filiberto.severi@unisi.it; Phone +39057758-6515; fax -3454

Felice Petraglia: felice.petraglia@unisi.it; Phone +39057723-3453; fax -3454

Davide Randazzo: davide.randazzo@unisi.it; Phone +39057723-4153; fax -4191

Daniela Rossi: daniela.rossi@unisi.it; Phone +39057723-4504; fax -4191

Vincenzo Sorrentino: vincenzo.sorrentino@unisi.it; Phone +39057723-4079; fax -4191

Running title: cultured smooth muscle pericytes

Corresponding author: Vincenzo Sorrentino, MD,
Department of Molecular and Developmental Medicine,
University of Siena, Via Aldo Moro 2, 53100 Siena, Italy,
e-mail: vincenzo.sorrentino@unisi.it; Phone: +39057723-4079; Fax: +39 057723-4191.

Abstract

Microvascular pericytes (PCs) are considered the adult counterpart of the embryonic mesoangioblasts, which represent a multipotent cell population that resides in the dorsal aorta of the developing embryo. Although PCs have been isolated from several adult organs and tissues, it is still controversial whether pericytes from different tissues exhibit distinct differentiation potentials. To address this point, we investigated the differentiation potentials of isogenic human cultured PCs isolated from skeletal (sk-hPCs) and smooth muscle tissues (sm-hPCs). We found that both sk-hPCs and sm-hPCs expressed known pericytic markers and did not express endothelial, hematopoietic and myogenic markers. Both sk-hPCs and sm-hPCs were able to differentiate into smooth muscle cells. In contrast, sk-hPCs, but not sm-hPCs, differentiated in skeletal muscle cells and osteocytes. Given the reported ability of the Notch pathway to regulate skeletal muscle and osteogenic differentiation, sk-hPCs and sm-hPCs were treated with DAPT, a known inhibitor of Notch signaling. DAPT treatment, as assessed by histological and molecular analysis, enhanced myogenic differentiation and abolished osteogenic potential of sk-hPCs. In contrast, DAPT treatment did not affect either myogenic or osteogenic differentiation of sm-hPCs. In summary, these results indicate that, despite of being isolated from the same anatomical niche, cultured pericytes from skeletal muscle and smooth muscle tissues display distinct differentiation abilities.

Abbreviations

ALP: alkaline phosphatase

at-hPCs: human adipose tissue cultured PCs

ct-hPCs: human cardiac tissue cultured PCs

DAPT: N-[N-(3,5-Difluorophenacetyl)-L-alanyl]-S-phenylglycine t-butyl ester

FC: flow cytometry

hMABs: human mesoangioblasts

MSCs: mesenchymal stem cells or marrow stromal cells

myomiRs: muscle specific miRNAs

NG2: neural/glial antigen 2

OSX: Osterix

PCs: pericytes

PDGFR- β : platelet-derived growth factor receptor- β

PW1/Peg3: PW1/paternally expressed gene 3

RT-PCR: reverse transcription polymerase chain reaction

RUNX2: Runt-related transcription factor 2

sk-hPCs: human skeletal muscle cultured PCs

SM22- α : smooth muscle protein-22 α

sm-hPCs: human smooth muscle cultured PCs

TAZ: PDZ-binding motif

TGF- β : transforming growth factor β

α -SMA: smooth muscle actin- α

Introduction

The maintenance of the homeostasis of human adult tissues is ensured by the presence of undifferentiated precursors that are able to replace those cells that are repeatedly lost following physiological, pathological or traumatic events. In addition to other tissue-specific stem cells found in tissues like blood, skin and gut [1], stem cells able to differentiate in the multiple cell types of mesodermal lineages have been identified in the connective tissue that forms the stromal compartment of most organs of the adult organism [2]. Mesenchymal progenitors, originally described in bone marrow [3] have been subsequently isolated from other organs [4-6]. These cells, known as mesenchymal stem cells (MSCs), are capable to differentiate in various types of connective cells such as osteocytes, adipocytes and chondrocytes [7]. MSCs are currently defined as multipotent cells that are obtained from the stromal portion of the tissues and further selected as plastic-adherent cells [8, 9]. However, mutual relations between mesenchymal progenitors of different tissues are still poorly understood and it is still unclear if cells with identical differentiation abilities can be isolated from all organs of the adult organism.

In the past years, following an alternative isolation procedure based on the harvesting of weak adhering cells emerging from explants-culture of vascularized connective portions of the tissues, a novel cell population endowed of multilineage mesodermal potential has been isolated from the skeletal muscle of mice, dogs and humans [10-12] and, subsequently, from the vascularized portion of additional human adult and fetal tissues [13]. These cells were further described, *in vivo*, among the endothelial-associated cells that contribute to the architecture of small blood vessels of organs and tissues and identified as perivascular pericytes (PCs) [14], strongly supporting the notion that the endothelium of the micro-vessels would represent the *in vivo* stem-niche of mesodermal adult progenitors [15-18]. The perivascular localization of PCs and their

multilineage differentiation abilities are in agreement with the hypothesis that these cells are the adult counterpart of the embryonic mesoangioblasts, which were firstly described as multipotent cells located in the dorsal aorta of the developing embryo [19]. Accordingly, it has been postulated that during organogenesis some mesoangioblasts migrate along the outgrowing blood vessels contributing to the formation of the perivascular cell compartment of post-natal tissues [15, 20].

Notably, adult PCs still express a subset of integrins and receptors that allows the efficient migration ability of these cells [21, 22]. Adult PCs from skeletal muscle have attracted attention because of their ability to differentiate in skeletal muscle cells and even more for their ability to cross the vascular wall, a feature that makes these cells particularly suitable for systemic cell-delivery in protocols of cell transplantation [23, 24]. PCs from human skeletal muscle are also able to differentiate towards additional lineages of mesodermal origin such as adipocytes, osteocytes and chondrocytes [12]. However, a comparative analysis of PCs from different human tissues indicated that PCs from skeletal muscle could differentiate towards mesodermal lineages more efficiently than PCs from adipose tissue [25]. In addition, PCs from adult heart are not able to differentiate into skeletal muscle cells but only into cardiac myocytes, adipocytes, osteocytes and chondrocytes [26]. These data suggest that, despite the proposed common embryonic origin and the localization at the same anatomical niche, namely the perivascular compartment, PCs from different tissues may show distinct differentiation abilities. Accordingly, a better understanding of the differentiation potentials of PCs from the different adult tissues is still necessary to further improve our current knowledge of the properties of these cells and to assess whether the multilineage potential of PCs may vary among different tissues.

In the present study, we compare the mesodermal differentiation abilities of isogenic human PCs isolated from skeletal (sk-hPCs) and smooth muscle (sm-hPCs). We report here that sm-hPCs differentiated only into smooth muscle cells, in contrast to the multilineage abilities of sk-hPCs. Inhibition of Notch signaling, which is known to regulate both myogenesis and osteogenesis [27-30], had no effect on the differentiation abilities of sm-hPCs. Conversely, inhibition of Notch signaling enhanced myogenic differentiation of sk-hPCs, while strongly reduced their osteogenic differentiation.

Materials and Methods

Cells isolation and culture

This study complies with the ethical standards laid down in the 1964 Declaration of Helsinki, and was approved by the local human investigation board.

Skeletal muscle and smooth muscle biopsies were obtained from 34 healthy pregnant women that underwent caesarian section and 8 women that underwent hysterectomy. Before enrollment, all woman signed a written informed consent at the Division of Obstetrics and Gynecology of “Policlinico Santa Maria alle Scotte” in Siena, Italy. Genetic and sampling variability were reduced by deriving isogenic pericytes from skeletal and smooth muscle biopsies from the same patient. All reagents were purchased from Sigma-Aldrich (St. Louis, MO, USA) if not otherwise specified. Pericytes were isolated as previously described [31]. Briefly, biopsies were cut in small pieces of about 1 mm³ and placed in collagen-coated Petri dishes at 37°C in humidified 5% CO₂ atmosphere. After at least four hours of adhesion, growing medium consisting of Dulbecco's Modified Eagle Medium (DMEM) MegaCell supplemented with 5% heat-inactivated Fetal Bovine Serum (FBS), 2 mM glutamine, 100 U/ml penicillin, 1% non-essential amino acids, 0.1 mM β-mercaptoethanol and 5 ng/ml basic fibroblast growth factor (Peprotech, Rocky Hill, NJ, USA), was added to the explants. After eight to twelve days from explant plating, floating and weakly adherent cells were poured out from the dishes and transferred to a new non-coated 100mm Petri dish. This step was considered as passage 1. From this step on, cell populations were maintained in culture, detached by trypsin/EDTA treatment when they reached 70%-80% of confluence, and transferred each time into uncoated 150mm Petri dishes at a plating density of 3000 cells/cm². At every passage, 1.5x10⁶ cells were harvested from a single 150mm Petri dish.

All the experiments described below were performed by passage five, on cells that did not exceed 20 population doublings.

Myogenic, osteogenic and adipogenic differentiation

Skeletal and smooth muscle differentiation were performed seeding 10,000 cells/cm² onto Matrigel (growth factor-reduced; BD, Franklin Lakes, NJ, USA) coated Petri dishes. After one day of adhesion, differentiation was induced by medium change. Skeletal muscle differentiation medium consisted of DMEM supplemented with 2% heat-inactivated horse serum (EuroClone, Picco, Milan, Italy), 2 mM glutamine, 1 mM sodium pyruvate (Lonza, Basel, Switzerland), 100 µg/ml streptomycin and 100 U/ml penicillin (D2 medium). Smooth muscle differentiation medium consisted of D2 medium supplemented with TGFβ 5 ng/ml (R&D, Minneapolis, MN, USA) freshly added every day. For the assessment of skeletal muscle differentiation, multinucleated myotubes were visualized both by DAPI and α-actinin staining ten days after induction of differentiation (see relevant paragraph). Fusion index of each cell population (n=6 for both sk-hPCs and sm-PCs) was calculated as the number of nuclei inside α-actinin positive myotubes, divided by the total number of nuclei in the relative microscopic field. Ten to twenty microscopic fields were randomly chosen among two different glass-slides. Each experiment was performed twice. For the assessment of smooth muscle differentiation, the presence of smooth muscle cells was verified by both SM22-α staining and α-SMA immunodetection (see relevant paragraphs) in differentiated cells, eight days after the induction of differentiation.

Osteogenic differentiation was performed by plating 20,000 cells/cm² onto uncoated Petri dishes. Cells were left to adhere for one day and then switched to the osteogenic medium consisting of Minimum Essential Medium alpha (α-MEM) supplemented of 10% heat inactivated FBS, 2 mM

L-glutamine, 100 U/ml penicillin, 100 µg/ml streptomycin, 0.1 µM dexamethasone, 50 µM ascorbate-2-phosphate and 10 mM β-glycerophosphate. Medium was changed every two days. Twenty-eight days after induction of differentiation, the production of extracellular calcified mineral matrix was visualized by Alizarin Red staining. Quantification of osteogenic differentiation was performed by the spectrophotometric evaluation of bound Alizarin Red dye as previously described [32].

Adipogenic differentiation was performed by plating 20,000 cells/cm² onto uncoated Petri dishes. The day after plating, differentiation was induced with adipogenic medium consisting of α-MEM supplemented with 10% heat-inactivated FBS, 2 mM L-glutamine, 100 µg/ml streptomycin, 100 U/ml penicillin, 0.5 mM isobutyl-methylxanthine, 1 µM dexamethasone, 10 µM insulin and 200 µM indomethacin. Medium was changed every two days. Fourteen days after plating, adipogenic differentiation was visualized by staining lipid droplets with Oil-red O. To quantify adipogenic differentiation, Oil-red O extraction was performed and spectrophotometrically evaluated as previously described [32].

Immunocytochemical analyses

Cells were fixed with 3% (v/v) paraformaldehyde in Phosphate Buffered Saline (PBS), permeabilized in Hepes/Triton buffer (20 mM Hepes pH 7.4, 300 mM sucrose, 50 mM NaCl, 3 mM MgCl₂, 0.5% Triton X-100), saturated with 10% FBS or normal goat serum (NGS) in PBS, and incubated 1 hour at room temperature with the following primary antibodies: monoclonal anti-α-actinin (1:1,000), polyclonal anti-SM22α (1:1,000, Abcam, Cambridge, UK), monoclonal anti-α-SMA (1:400), monoclonal anti-desmin (1:1,000, Millipore, Temecula, CA), monoclonal anti-MyoD (1:50, Abcam), monoclonal anti-myogenin (1:150, Abcam). Rhodamine-conjugated

phalloidin (1:1,000, Thermo Fisher Scientific, Waltham, MA, USA) was used to reveal F-actin cytoskeleton. To reveal bound primary antibodies, cells were incubated for 1 hour at room temperature with specific secondary antibodies (anti-mouse IgG conjugated to cyanine2, 1:5,000; anti-mouse IgG conjugated to cyanine3, 1:5,000; anti-goat IgG conjugated to cyanine3, 1:2,000, all from Jackson Laboratories, Bar Harbor, ME, USA). Mouse monoclonal anti- α -actinin and mouse monoclonal anti-myogenin antibodies were directly conjugated to the relevant fluorochrome using Alexa Fluor 647 Monoclonal antibody labeling kit (Molecular Probes, Life Technologies, Waltham, MA, USA) and Alexa Fluor 488 Zenon mouse IgG labeling kit (Invitrogen, Life Technologies, Waltham, MA, USA), according to manufacturer's instruction. Nuclei were visualized by 4',6-diamidino-2-phenylindole (DAPI, 1:10,000 Calbiochem, San Diego, CA, USA) or TO-PRO[®]-3 Iodide (1:1,000, Molecular Probes) staining. Slides were analyzed with LSM-510 META confocal microscope (Carl Zeiss, Oberkochen, Germany).

DAPT treatment

The cleavage of Notch intracellular domain was inhibited by adding N-[N-(3,5-Difluorophenacetyl)-L-alanyl]-S-phenylglycine t-butyl ester (DAPT), a selective inhibitor of γ -secretase [33], to proliferation and/or differentiation medium, at a final concentration of 20 μ M. DAPT was re-suspended in dimethyl sulfoxide (DMSO). Accordingly, all control cell populations used for the comparative analysis were cultured in the presence of equal amount of DMSO. DAPT and DMSO treatment was performed for two consecutive passages (p3 and p4) on undifferentiated growing cells. During myogenic, osteogenic and adipogenic differentiation, DAPT and DMSO were freshly added at every medium change.

Total RNA and miRNA extraction, cDNA synthesis and PCR analysis

Total RNA and microRNA were extracted from either undifferentiated and differentiating cells using miRNeasy Mini kit (Qiagen, Hilden, Germany), following manufacturer's instructions. MicroRNA fraction was enriched using RNeasy® MinElute™ Cleanup Kit (Qiagen). RNA and microRNA concentration was evaluated with NanoDrop ND-1000 Spectrophotometer (Thermo Fisher Scientific). 200 ng of total RNA was reverse-transcribed using the M-MLV Reverse Transcriptase (Promega, Fitchburg, WI, USA) following the manufacturer's instructions.

MicroRNAs were converted into double-strand cDNA with the miScript II RT kit (Qiagen), following manufacturer's instructions.

Quantitative real-time PCR analysis was performed on StepOnePlus™ detection system (Applied Biosystems, Waltham, MA, USA). Power SYBR® PCR Master Mix (Applied Biosystems) were used to amplify the cDNA from total RNA and QuantiTect SYBR® Green PCR Master Mix was used to amplify microRNAs (Qiagen). All Ct values greater than 35 were not considered. The relative RNA and microRNA expressions were calculated using β -actin and hsa-RNU6-2 (Qiagen) as internal control, respectively, according to Pfaffl's $2^{-\Delta\Delta Ct}$ quantification method [34].

Primers used were as follows:

PDGFR- β : Fw CAGTAAGGAGGACTTCCTGGAG; Rev CCTGAGAGATCTGTGGTTCCAG;

ALP: Fw CTCCTCGGAAGACACTCTG; Rev CACCACCTTGTAGCCAGGCC;

MYOD: Fw GAAGCTAGGGGTGAGGAAGC; Rev CCCGGCTGTAGATAGCAAAG;

MYF5: Fw CTATAGCCTGCCGGGACA; Rev TGGACCAGACAGGACTGTTACAT;

β -ACTIN: Fw CAACTCCATCATGAAGTGTGAC Rev GCCATGCCAATCTCATCTTG;

TAZ: Fw AGATGACCTTCACGGCCACTG; Rev TGAGGCACTGGTGTGGAAGT

RUNX2: Fw GCAGCAGCTATTAAATCCAA; Rev ACAGATTCATCCATTCTGCCA;

OSX: Fw GCCAGAAGCTGTGAAACCTC; Rev GCAACAGGGGATTAACCTGA;

PW1/PEG3: Fw GATCCAAGAGAAGTGCCTACC; Rev

GGAAGATTCATCTTCACAAATCCC);

hsa-miR-1: UGGAAUGUAAAGAAGUAUGUAU;

hsa-miR-133b:UUUGGUCCCCUUAACCAGCUA;

has-miR-206:UGGAAUGUAAGGAAGUGUG UGG.

Protein extraction and western blot

Cell pellets were lysed for 30 minutes at 4°C using RIPA buffer (TRIS 50 mM, NaCl 150 mM, SDS 0.1 %, sodium deoxycholate 0.5 %, Triton X-100 or NP40 1 %) supplemented with protease inhibitor cocktail. Centrifugation at 11,000 rcf for 10 minutes at 4°C allowed the removal of insoluble materials. Protein concentration was assessed using Bradford protein assay (Bio-Rad, Hercules, CA). 50 µg of total proteins were loaded on 12.5% SDS–polyacrylamide electrophoresis gel. Separated proteins were transferred onto PVDF membrane that was blocked with 5% non-fat-milk in TRIS-buffered saline and Tween 20 for 1 hour at RT. Primary antibody incubation was performed overnight at 4°C with the following antibodies: polyclonal anti-NG2 (1:500; Chemicon, EMD Millipore, Billerica, MA, USA), monoclonal anti-desmin (1:3,000, Millipore), monoclonal anti- α -tubulin (1:5,000), polyclonal anti-SM22- α (1:5,000, Abcam), monoclonal anti- α SMA (1:2,000). Secondary anti-rabbit-, anti-mouse- and anti-goat-IgG antibodies conjugated to horseradish peroxidase (1:3,000, Ge-Healthcare, Little Chalfont, UK) were kept 1 hour at RT. Immunoreactive bands were detected using Amersham ECL Western Blotting Detection Reagent (Ge-Healthcare). Quantification of the intensities of immunoreactive bands was performed by ImageJ software (National Institutes of Health).

Flow cytometry

Flow cytometry (FC) analysis was performed on undifferentiated cells at early passages (p2-p5). Cells were collected by trypsinization and then washed in ice-cold PBS containing 0.5% Bovine Serum Albumin (BSA) (FC buffer). 1×10^5 cells were re-suspended in FC buffer and incubated for 30 minutes at 4°C with the following monoclonal antibodies: phycoerythrin (PE)-conjugated CD13 (1:50, DAKO, Agilent Technologies, Santa Clara, CA, USA); PE-conjugated CD31 (1:50, Santa Cruz, Dallas, TX, USA); allophycocyanin (APC)-conjugated CD34 (1:50, BD, Franklin Lakes, NJ, USA); APC-conjugated CD44 (1:50, e-Bioscience, San Diego, CA, USA); fluorescein isothiocyanate (FITC)-conjugated CD45 (1:50, BD); CD73 (1:50, BD); APC-conjugated CD90 (1:50, BD); PE-conjugated CD105 (1:50, Ancell, Bayport, MN, USA); PE-conjugated CD146 (1:50, BD); FITC-conjugated NG2 (1:50, e-Bioscience). PE-conjugated anti-mouse IgG secondary antibody (1:50, BD) was used for the detection of CD73 positive cells. To set fluorescence background, identical Ig isotypes conjugated to PE, FITC or APC (all from BD) were used.

Statistical analysis

Statistical analysis was performed using the Student's t-test or the two-way analysis of variance using GraphPad Prism6 software. Wilcoxon matched-pair non parametric T-test was used to compare microRNAs expression during myogenic differentiation of given cell populations, setting target expression of undifferentiated cells as internal reference. Mann-Whitney unpaired non parametric T-test was used to compare microRNAs expression between isogenic sk-hPCs and sm-hPCs during both proliferation and differentiation, setting target expression of sk-hPCs as internal reference. Results are presented as mean \pm SEM of at least three different pairs of

isogenic sk-hPCs and sm-hPCs. Differences in target expression were considered statistically significant when p -value was lower than 0.05 ($p < 0.05$).

Results

Sk-hPCs and sm-hPCs have comparable immunophenotype and molecular pattern

Biopsies from skeletal and smooth muscle were obtained from the same patients and were processed in parallel to isolate isogenic sk-hPCs and sm-hPCs from 42 donors, exploiting a previously reported isolation procedure [31]. All data presented throughout the manuscript are from six representative isogenic sk-hPCs and sm-hPCs (donors #1, #2, #5, #6: caesarian section; donors #3, #4: hysterectomy). The remaining 36 isogenic pairs were also analyzed and gave similar results. Cells were expanded for two/three passages, and morphologically indistinguishable (Fig. 1B) sk-hPCs and sm-hPCs were analyzed in parallel to assess the presence of pericytic markers and the absence of both endothelial and myogenic markers. Flow cytometry analysis indicated that all cell populations stained positive for the surface antigens CD13, CD44, CD146 and neural/glial antigen 2 (NG2) (Fig. 1A), in agreement with previously reported analysis on *in vitro* [12, 25] and *in vivo* [13] microvascular pericytes from skeletal muscle and adipose tissue. The percentage of cells expressing CD146 and NG2 varied across cell populations, ranging between 12-71% and 48-85%, respectively. Variable expression of NG2 across cell populations was also noted in Western blot experiments (Fig. 1D). In addition, mesenchymal immunophenotype of sk-hPCs and sm-hPCs was corroborated by the expression of CD73, CD90 and CD105 (Fig 1A). Finally, the endothelial and/or hematopoietic markers CD31, CD34 and CD45 were never detected (Fig. 1A). To further confirm that isolated cells expressed microvascular pericytes' markers, expression of platelet-derived growth factor receptor- β (PDGFR- β) and alkaline phosphatase (ALP), two markers expressed by vessel-associated pericytes [35], was verified by RT-PCR in all sk-hPCs and sm-hPCs (Fig. 1C). Conversely, the

expression of myogenic factors such as MYOD and MYF5 was never detected (Fig. 1C).

Western blot analysis indicated that all sk-hPCs and sm-hPCs expressed desmin (Fig. 1D), whose expression was also confirmed by immunofluorescence analysis (Fig 1E, a-d). Finally, all cell populations expressed smooth muscle actin- α (α -SMA), although different levels of expression and pattern of organization were noted in sm-hPCs (Fig. 1E, e-h and 2B, a).

Sk-hPCs and sm-hPCs have distinct differentiation potentials

Smooth muscle, osteogenic and adipogenic potentials of isogenic sk-hPCs and sm-hPCs were evaluated to assess the multi-potential properties of the isolated cell populations. Smooth muscle differentiation was induced by continuous transforming growth factor- (TGF-) β treatment for eight days. Both sk-hPCs and sm-hPCs were able to differentiate in smooth muscle cells as confirmed by the expression of smooth muscle protein-22 α (SM22- α) and α -SMA (Fig. 2A, a-l and 2B, a). Both smooth muscle markers were up-regulated following eight days of differentiation (Fig. 2B, b).

All sk-hPCs exposed to osteogenic medium differentiated in calcified mineral matrix-secreting cells as early as fifteen days following the induction of osteogenic differentiation, as assessed by Alizarin-Red staining (Fig 2C, a-f). In marked contrast, sm-hPCs were not able to secrete extracellular ossified mineral matrix even twenty-eight days after the induction of differentiation (Fig. 2C g-l).

Finally, sk-hPCs readily differentiated into adipocytes, as revealed by Oil Red-O staining of lipid droplets into the cytoplasm (Fig. 2D, a-f). In contrast, sm-hPCs were not able to accumulate lipid droplets, indicating that they failed adipogenic differentiation (Fig. 2D, g-l).

Sk-hPCs but not sm-hPCs differentiate in skeletal muscle cells

The myogenic potential of sk-hPCs has attracted the interest of several researchers given the potential clinical application of these cells. In fact, sk-hPCs are currently used in a phase I/II clinical trial aimed to ameliorate the conditions of patients affected by Duchenne muscular dystrophy (EudraCT n° 2011-000176-33). To better understand if skeletal myogenic potential is confined to skeletal muscle pericytes or it is also a property of pericytes residing in other tissues, we performed a more detailed analysis of skeletal muscle differentiation, comparing sk-hPCs and sm-hPCs. Undifferentiated cells were thus exposed to skeletal muscle-differentiation medium for ten days. Sk-hPCs fused and formed multinucleated α -actinin positive myotubes (Fig 3A, a-f) that were already formed as early as seven days after the induction of differentiation (Fig. 3B, g-i). In contrast, sm-hPCs did not fuse and α -actinin positive cells were never detected during the same time-course of differentiation (Fig. 3A, j-l). To exclude a mere delay of myogenesis in differentiating sm-hPCs, skeletal muscle differentiation was carried on for five additional days. Nonetheless, even following fifteen days of differentiation, sm-hPCs were still unable to fuse and form myotubes (Fig. 3B, p-r). Similarly, neither α -actinin positive cells nor multinucleated myotubes were observed when sm-hPCs were even co-cultured with the mouse C2C12 cells (data not shown), which enhance the ability of human adipose tissue-derived pericytes to form myotubes [25].

Skeletal myogenic differentiation relies on a fine tuned mechanism based on the interplay between known myogenic factors, including MyoD and Myogenin, and a recently identified set of muscle-specific microRNAs, called myomiRs [36]. Interestingly, following the exposure to myogenic medium, the expected sequential activation of MyoD and Myogenin was observed in

differentiating sk-hPCs (Fig 3B, a-c and g-i) while no expression of MyoD and Myogenin was observed in sm-hPCs (Fig. 3B, d-f and j-l). We also analyzed the expression of three major pro-myogenic myomiRs, namely mir-1, mir-133b and mir-206, during the early phases of myogenic differentiation of both sk-hPCs and sm-hPCs. As expected, the expression of mir-1, mir-133b and mir-206 was up-regulated in differentiating sk-hPCs, while the expression of the three myomiRs was unaffected or even decreased in sm-hPCs induced to differentiate (Fig. 3C). Accordingly, direct comparison of myomiRs expression between sk-hPCs and sm-hPCs showed that sk-hPCs displayed higher expression level of mir-1, mir-133b and mir-206 with respect to sm-hPCs in both undifferentiated and differentiating conditions (Fig. 3D). Finally, we also found that the expression of PW1/Peg3, recently identified as a key regulator of human mesoangioblasts stem cell competence [37], was reduced by about 50% in sm-hPCs with respect to the levels observed in sk-hPCs, in agreement with the results obtained from differentiation analysis of sk-hPCs and sm-hPCs (Fig 3E).

Notch signaling inhibition affects sk-hPCs but not sm-hPCs differentiation abilities

The results obtained from the differentiation analysis of sk-hPCs and sm-hPCs indicated that cultured pericytes isolated from skeletal and smooth muscle tissues are endowed with distinct differentiation abilities, although they can be isolated from the micro-vascularized portion of the tissues and share similar immunophenotypic and molecular pattern. Given the ability of Notch to regulate and direct myogenic and osteogenic potential of undifferentiated cells [27-30], we next investigated whether the inhibition of Notch signaling would affect the differentiation potential of sk-hPCs and sm-hPCs. Accordingly, isogenic sk-hPCs and sm-hPCs were cultured in the presence of DAPT, a selective inhibitor of γ -secretase [33], for two consecutive passages, before

the induction of differentiation. Following DAPT addition for two passages, we observed a three-fold reduction of the amount of Notch intracellular domain in treated cells, as assessed by Western blot analysis (data not shown). Cells were then induced to differentiate towards myogenic and osteogenic lineages in the presence of DAPT. The inhibition of Notch signaling during both proliferation and differentiation of sk-hPCs enhanced the recruitment of nuclei into myotubes (Fig.4A, a,b), resulting in a three-fold increase of overall fusion index compared to untreated cell populations (Fig. 4A, c). Accordingly, the expression of the early myogenic factors MYOD and MYF5 (Fig. 4C) and the expression of pro-myogenic microRNAs, mir-1, mir-133b, and mir-206 (Fig. 4D) were significantly up-regulated in DAPT-treated sk-hPCs. Interestingly, the enhancement of myogenic efficiency of DAPT-treated sk-hPCs was effective only when DAPT was continuously administered in both growth and differentiation media. In fact, either DAPT treated-undifferentiated sk-hPCs induced to differentiate in the absence of DAPT, and untreated undifferentiated sk-PCs induced to differentiate in the presence of DAPT did not display altered fusion index with respect to control cells (Fig. 4E). At variance of sk-hPCs, all DAPT-treated sm-hPCs remained unable to fuse and form myotubes (Fig. 4B, a-c). Accordingly, the expression of MYOD, MYF5, mir-1, mir-133b and mir-206 in sm-hPCs was unaffected by drug treatment (data not shown).

The effect of DAPT treatment on the osteogenic potential of sk-hPCs and sm-hPCs was also investigated. The ability of sk-hPCs to differentiate towards osteogenic lineage was strongly reduced following continuous DAPT treatment during both proliferation and differentiation (Fig. 5A, a,b). Quantitative analysis of cell differentiation performed by means of Alizarin-Red extraction, indicated that the amount of extracellular mineral matrix produced by DAPT-treated sk-hPCs was about twenty fold lower than that measured in untreated sk-hPCs (Fig 5A, c).

Accordingly, quantitative RT-PCR analysis of transcription factors involved in the onset of osteogenic differentiation such as transcriptional coactivator with PDZ-binding motif (TAZ), Runt-related transcription factor 2 (RUNX2) and Osterix (OSX) revealed that the expression of all these genes was significantly down-regulated following DAPT treatment. Interestingly, DAPT was able to inhibit osteogenesis of sk-hPCs when present only during differentiation. Addition of DAPT to only undifferentiated cells was not sufficient to inhibit osteogenesis (Fig. 5D). Finally, the analysis of Notch signaling inhibition on osteogenic potential of sm-hPCs revealed that DAPT treated sm-hPCs were not able to differentiate towards osteogenic lineage, in strict analogy with the results obtained with untreated sm-hPCs (Fig. 5B, a-c and 2C, g-l). The effect of DAPT treatment on sk-hPCs and sm-hPCs was also assessed on adipogenic differentiation. Notch signaling inhibition did not alter the adipogenic potential of both cell populations, yielding results comparable to those obtained from control cell populations (data not shown and Fig 2D, a-l).

Discussion

Multilineage mesodermal differentiation potential has been proven for human PCs isolated from skeletal muscle (sk-hPCs), adipose (at-hPCs) and cardiac (ct-hPCs) adult tissues [12, 13, 26].

However, whether hPCs from distinct tissues are equivalent in terms of differentiation abilities is not yet clear. To further address this point, cultured pericytes derived from smooth muscle (sm-hPCs) were compared to isogenic sk-hPCs. Based on the initial characterization reported in Fig. 1, we concluded that sk-hPCs and sm-hPCs share the same immunophenotypic and molecular profile. According to previous data on PCs from adipose tissue [25], these findings indicate that cultured pericytes isolated from different sources without exploiting any additional cell-selection, are virtually indistinguishable. However, when we compared multipotent differentiation abilities of sk-hPCs and sm-hPCs, we observed that sk-hPCs were able to differentiate into adipocytes, osteocytes, skeletal and smooth muscle cells, while sm-hPCs were only able to give rise to smooth muscle cells. The restricted differentiation abilities of sm-hPCs is surprising compared to those of sk-hPCs, at-hPCs or ct-hPCs, where at least adipogenic and osteogenic potentials have been always observed [12, 13, 26]. Interestingly, stem cells from myometrium endowed with adipogenic, osteogenic and chondrogenic differentiation abilities, and thus resembling putative MSCs, have been reported [38]. However, sm-hPCs and myometrial MSCs differ in their morphology, molecular marker profiles and differentiation abilities. Notably, such differences are not observed in adipose tissue where both MSCs and PCs are capable to differentiate into smooth muscle cells but also into adipocytes and osteocytes.

Lack of multipotent abilities of sm-hPCs with respect to sk-hPCs is in agreement with a recent report showing that cardiac pericytes, although able to differentiate towards osteocytes and adipocytes, fail to differentiate in skeletal muscle cells [26]. In addition, we recently reported that

hPCs isolated from skeletal and adipose tissues are yet endowed with multipotent mesodermal abilities, but sk-hPCs differentiate at much more efficient rate than at-hPCs [25]. Taken together, all these evidences indicate that hPCs isolated from different tissues cannot be considered equivalent in terms of their differentiation potentials.

It has been recently shown that stem cell competence of adult sk-hPCs, and in particular their skeletal myogenic potential, is positively regulated by the expression of PW1/Peg3 [37]. The authors also showed that knockdown of PW1/Peg3 abrogated skeletal muscle differentiation of human mesoangioblasts. PW1/Peg3 expression has been also detected in PICs (PW1+/Pax7- interstitial cells), a myogenic cell population apparently distinct from pericytes, which has been identified in the interstitium of post-natal skeletal muscle [39], and that is also able to support skeletal myogenesis of satellite cells [40]. Here, we report that PW1/Peg3 expression in sm-hPCs is only about 50% of that observed in sk-hPCs. Why sm-hPCs, although able to express considerable levels of PW1/Peg3, are unable to differentiate into skeletal muscle cells remains to be determined.

It is worth noting that spontaneous differentiation into skeletal muscle cells has been observed only in sk-hPCs. In fact, skeletal muscle differentiation of at-hPCs, even if not as efficient as that of sk-hPCs, was dependent on co-culture with rodent myoblasts [25]. On the other hand, sm-hPCs were not able to differentiate into skeletal muscle cells even following induction of differentiation in co-culture with C2C12 cells (data not shown). Furthermore, inhibition of Notch signaling, known to stimulate skeletal muscle differentiation of myogenic cells [41], was unable to stimulate skeletal myogenic differentiation in sm-hPCs. This agrees with molecular analysis revealing that sm-hPCs, at variance of sk-hPCs, were not able, upon induction of skeletal muscle differentiation, to activate the expression of myogenic transcription factors or muscle specific

microRNAs such as mir-1, mir-133b and mir-206, further confirming that sm-hPCs do not have any potential to differentiate into skeletal muscle cells. Interestingly, failure of both cardiac and adipose tissue pericytes to undergo spontaneous myogenic differentiation has also been linked to lack of coordinated expression of MyoD, Myf5 and muscle specific microRNAs [25, 42].

Notably, we observed that skeletal myogenic differentiation of sk-hPCs was enhanced by inhibition of Notch signaling, in agreement with previous studies on murine C2C12 and satellite cells [41, 43-45]. Here, we provide evidence that Notch pathway inhibition enhances skeletal myogenic differentiation of sk-hPCs acting on the regulation of the expression of myogenic factors and myomiRs. This, however, contrasts with a recent study reporting that alkaline phosphatase (AP)-positive human mesoangioblasts (hMABs) require Dll1-induced canonical Notch signaling to achieve a more efficient skeletal muscle differentiation [46]. These apparently conflicting results might reflect the isolation protocol used by Quattrocchi and co-workers [46], which selects a subpopulation of ALP-positive cells from the bulk cell population of hPCs used in their work. Indeed, the effective role of Notch signaling in skeletal muscle differentiation still needs to be fully elucidated [47]. Interestingly, we also found that Notch signaling inhibition completely abolished osteogenic potential of sk-hPCs. To our knowledge, this is the first study that describes the effect of inhibition of Notch pathway on the osteogenic fate of adult sk-hPCs. Different reports show that Notch signaling is a regulator of osteogenic differentiation [29, 30] although opposite effects, likely depending on cell types and/or temporal context and stage of commitment, have been reported [48-50].

In conclusion, the results reported in this study support the notion that hPCs from different adult tissues, even when isolated using the same protocol, show distinct differentiation potentials.

Skeletal muscle PCs can spontaneously differentiate into skeletal muscle cells, but also in

osteocytes, adipocytes and smooth muscle cells. Human PCs from adipose and cardiac tissues are able to differentiate into osteocytes, adipocytes and smooth muscle cells. Pericytes from adipose tissue can differentiate into muscle cells, but only when co-cultured with myogenic cells. As reported here, hPCs from myometrium display only a restricted unipotent potential to differentiate toward smooth muscle cells. Further work will help to define whether this restricted potential may reflect the acquisition of physiological features of myometrial cells, like those observed in pregnancy. This latter aspect agrees with the emerging hypothesis that the hPCs may be committed and recruited to fulfill the specific growth and/or repair requirements of the tissue where they reside [51, 52].

Acknowledgments

This work was supported by a grant from “Regione Toscana” to Vincenzo Sorrentino and a MIUR-FIR 2013 RBFR13A20K grant to Enrico Pierantozzi.

Author Disclosure Statement

The authors declare no competing financial interests.

References

- 1 Goodell MA, H Nguyen and N Shroyer. (2015). Somatic stem cell heterogeneity: diversity in the blood, skin and intestinal stem cell compartments. *Nat Rev Mol Cell Biol* 16:299-309.
- 2 Da Silva Meirelles L, PC Chagastelles and NB Nardi. (2006). Mesenchymal stem cells reside in virtually all post-natal organs and tissues. *J Cell Sci* 119:2204-2213.
- 3 Pittenger MF, AM Mackay, SC Beck, RK Jaiswal, R Douglas, JD Mosca, MA Moorman, DW Simonetti, S Craig and DR Marshak. (1999). Multilineage potential of adult human mesenchymal stem cells. *Science* 284:143–147.
- 4 Zuk PA, M Zhu, H Mizuno, J Huang, JW Futrell, AJ Katz, P Benhaim, HP Lorenz and MH Hedrick. (2001). Multilineage cells from human adipose tissue: implications for cell-based therapies. *Tissue Eng* 7:211-228.
- 5 Beltrami AP, D Cesselli, N Bergamin, P Marcon, S Rigo, E Puppato, F D'Aurizio, R Verardo, S Piazza, A Pignatelli, A Poz, U Baccarani, D Damiani, R Fanin, L Mariuzzi, N Finato, P Masolini, S Burelli, O Belluzzi, C Schneider and CA Beltrami. (2007). Multipotent Cells can be generated in vitro from several Adult Human Organs (Heart, Liver and Bone Marrow). *Blood* 110:3438-3446.

- 6 Gallo R, F Gambelli, B Gava, F Sasdelli, V Tellone, M Masini, P Marchetti, F Dotta and V Sorrentino. (2007). Generation and expansion of multipotent mesenchymal progenitor cells from cultured human pancreatic islets. *Cell Death Differ* 14:1860-1861.
- 7 Khan WS and TE Hardingham. (2012). Mesenchymal stem cells, sources of cells and differentiation potential. *J Stem Cells* 7:75-85.
- 8 Sousa BR, RC Parreira and EA Fonseca. (2014). Human adult stem cells from diverse origins: an overview from multiparametric immunophenotyping to clinical applications. *Cytometry A* 85:43-77.
- 9 Lv FJ, RS Tuan, KM Cheun and VY Leung. (2014). Concise review: the surface markers and identity of human mesenchymal stem cells. *Stem Cells* 32:1408-1419.
- 10 Minasi MG, M Riminucci, L De Angelis, U Borello, B Berarducci, A Innocenzi, A Caprioli, D Sirabella, M Baiocchi, R De Maria, R Boratto, T Jaffredo, V Broccoli, P Bianco and G Cossu. (2002). The meso-angioblast: a multipotent, self renewing cell that originates from the dorsal aorta and differentiates into most mesodermal tissues. *Development* 129:2773–2783.
- 11 Sampaolesi M, S Blot, G D'Antona, N Granger, R Tonlorenzi, A Innocenzi, P Mognol, JL Thibaud, BG Galvez, I Barthélémy, L Perani, S Mantero, M Guttinger, O Pansarasa, C Rinaldi, MG Cusella De Angelis, Y Torrente, C Bordinon, R Bottinelli and G Cossu.

- (2006). Mesoangioblast stem cells ameliorate muscle function in dystrophic dogs. *Nature* 444:574–579.
- 12 Dellavalle A, M Sampaolesi, R Tonlorenzi, E Tagliafico, B Sacchetti, L Perani, A Innocenzi, BG Galvez, G Messina, R Morosetti, S Li, M Belicchi, G Peretti, JS Chamberlain, WE Wright, Y Torrente, S Ferrari, P Bianco and G Cossu. (2007). Pericytes of human skeletal muscle are myogenic precursors distinct from satellite cells. *Nat Cell Biol* 9:255–267.
 - 13 Crisan M, S Yap, L Casteilla, CW Chen, M Corselli, TS Park, G Andriolo, B Sun, B Zheng, L Zhang, C Norotte, PN Teng, J Traas, R Schugar, BM Deasy, S Badylak, HJ Buhring, JP Giacobino, L Lazzari, J Huard and B Péault. (2008). A perivascular origin for mesenchymal stem cells in multiple human organs. *Cell Stem Cell* 3:301-313.
 - 14 Crisan M, CW Chen, M Corselli, G Andriolo, L Lazzari and B Péault. (2009). Perivascular Multipotent Progenitor Cells in Human Organs. *Hematopoietic Stem Cells VII: Ann NY Acad Sci* 1176:118–123.
 - 15 Bianco P and G Cossu. (1999). Uno, nessuno e centomila: Searching for the Identity of Mesodermal Progenitors. *Exp Cell Res* 251:257–263.
 - 16 Cossu G and P Bianco. (2003). Mesoangioblasts-vascular progenitors for extravascular mesodermal tissues. *Curr Opin Genet Dev* 13:537-542.

- 17 Crisan M, M Corselli, CW Chen and B Péault. (2011). Multilineage stem cells in the adult: a perivascular legacy? *Organogenesis*. 7:101-104.
- 18 Murray IR, CC West, WR Hardy, AW James, TS Park, A Nguyen, T Tawonsawatruk, L Lazzari, C Soo and B Péault. (2014). Natural history of mesenchymal stem cells, from vessel walls to culture vessels. *Cell Mol Life Sci* 71:1353-1374.
- 19 De Angelis L, L Berghella, M Coletta, L Lattanzi, M Zanchi, MG Cusella-De Angelis, C Ponzetto and G Cossu. (1999). Skeletal Myogenic Progenitors Originating from Embryonic Dorsal Aorta Coexpress Endothelial and Myogenic Markers and Contribute to Postnatal Muscle Growth and Regeneration. *J Cell Biol* 147:869–877.
- 20 Bianco P, PG Robey and PJ Simmons. (2008). Mesenchymal Stem Cells: Revisiting History, Concepts, and Assays. *Cell Stem Cell* 2:313–319.
- 21 Tagliafico E, S Brunelli, A Bergamaschi, L De Angelis, R Scardigli, D Galli, R Battini, P Bianco, S Ferrari and G Cossu. (2004). TGF β /BMP activate the smooth muscle/bone differentiation programs in mesoangioblasts. *J Cell Sci* 117:4377-4388.
- 22 Aguilera KY and RA Brekken. (2014). Recruitment and retention: factors that affect pericyte migration. *Cell Mol Life Sci* 71:299–309.

- 23 Tedesco FS, A Dellavalle, J Diaz-Manera, G Messina and G Cossu. (2010). Repairing skeletal muscle: regenerative potential of skeletal muscle stem cells. *J Clin Invest* 120:11–19.
- 24 Crisan M, M Corselli, WC Chen and B Péault. (2012). Perivascular cells for regenerative medicine. *J Cell Mol Med* 12:2851-2860.
- 25 Pierantozzi E, M Badin, B Vezzani, C Curina, D Randazzo, F Petraglia, D Rossi and V Sorrentino. (2015). Human pericytes isolated from adipose tissue have better differentiation abilities than their mesenchymal stem cell counterparts. *Cell Tissue Res* 361:769-778.
- 26 Chen WC, JE Baily, M Corselli, ME Díaz, B Sun, G Xiang, GA Gray, J Huard and B Péault. (2015). Human myocardial pericytes: multipotent mesodermal precursors exhibiting cardiac specificity. *Stem Cells* 33:557-573.
- 27 Bjornson CR, TH Cheung, L Liu, PV Tripathi, KM Steeper and TA Rando. (2012). Notch signaling is necessary to maintain quiescence in adult muscle stem cells. *Stem Cells* 30:232-242.
- 28 Fukada S, M Yamaguchi, H Kokubo, R Ogawa, A Uezumi, T Yoneda, MM Matev, N Motohashi, T Ito, A Zolkiewska, RL Johnson, Y Saga, Y Miyagoe-Suzuki, K Tsujikawa, S Takeda and H Yamamoto. (2011). *Hesr1* and *Hesr3* are essential to generate

undifferentiated quiescent satellite cells and to maintain satellite cell numbers.

Development 138:4609-4619.

- 29 Sciaudone M, E Gazzo, L Priest, AM Delany and E Canalis. (2003). Notch 1 Impairs Osteoblastic Cell Differentiation. *Endocrinology* 144:5631–5639.
- 30 Shindo K, N Kawashima, K Sakamoto, A Yamaguchi, A Umezawa, M Takagi, K Katsube and H Suda. (2003). Osteogenic differentiation of the mesenchymal progenitor cells, Kusa is suppressed by Notch signaling. *Exp Cell Res* 290:370–380.
- 31 Tonlorenzi R, A Dellavalle, E Schnapp, G Cossu and M Sampaolesi. (2007). Isolation and characterization of mesoangioblasts from mouse, dog, and human tissues. *Curr Protoc Stem Cell Biol* Chapter 2:Unit 2B 1.
- 32 Manini I, L Gulino, B Gava, E Pierantozzi, C Curina, D Rossi, A Brafa, C D'Aniello and V Sorrentino. (2011). Multi-potent progenitors in freshly isolated and cultured human mesenchymal stem cells: a comparison between adipose and dermal tissue. *Cell Tissue Res* 344:85–95.
- 33 Geling A, H Steiner, M Willem, L Bally-Cuif and C Haass. (2002). A γ -secretase inhibitor blocks Notch signaling in vivo and causes a severe neurogenic phenotype in zebrafish. *Embo Rep* 3:688-694.

- 34 Pfaffl MW. (2001). A new mathematical model for relative quantification in real time RT-PCR. *Nucleic Acids Res* 29:e45.
- 35 Quattrocelli M, G Palazzolo, I Perini, S Crippa, M Cassano and M Sampaolesi. (2012). Mouse and human mesoangioblasts: isolation and characterization from adult skeletal muscles. *Methods Mol Biol* 798:65-76.
- 36 Braun T and M Gautel. (2011). Transcriptional mechanisms regulating skeletal muscle differentiation, growth and homeostasis. *Nat Rev Mol Cell Biol* 12:349-361.
- 37 Bonfanti C, G Rossi, FS Tedesco, M Giannotta, S Benedetti, R Tonlorenzi, S Antonini, G Marazzi, E Dejana, D Sassoon, G Cossu and G Messina. (2015). PW1/Peg3 expression regulates key properties that determine mesoangioblast stem cell competence. *Nat Commun* 2015; 6:6364.
- 38 Ono M, T Maruyama, H Masuda, T Kajitani, T Nagashima, T Arase, M Ito, K Ohta, H Uchida, H Asada, Y Yoshimura, H Okano and Y Matsuzaki. (2007). Side population in human uterine myometrium displays phenotypic and functional characteristics of myometrial stem cells. *PNAS* 104:18700-18705.
- 39 Mitchell KJ, A Pannérec, B Cadot, A Parlakian, V Besson, ER Gomes, G Marazzi and DA Sassoon. (2010). Identification and characterization of a non-satellite cell muscle resident progenitor during postnatal development. *Nat Cell Biol* 12:257-266.

- 40 Pannerec A, G Marazzi and D Sassoon. (2012). Stem cells in the hood: the skeletal muscle niche. *Trends Mol Med* 18:599-606.
- 41 Conboy MI and TA Rando. (2002). The regulation of Notch signaling controls satellite cell activation and cell fate determination in postnatal myogenesis. *Dev Cell* 3:397–409.
- 42 Crippa S, M Cassano, G Messina, D Galli, BG Galvez, T Curk, C Altomare, F Ronzoni, J Toelen, R Gijsbers, Z Debyser, S Janssens, B Zupan, A Zaza, G Cossu and M Sampaolesi. (2011). miR669a and miR669q prevent skeletal muscle differentiation in postnatal cardiac progenitors. *J Cell Biol* 193:1197-121.
- 43 Buas MF, S Kabak and T Kadesch. (2009). Inhibition of Myogenesis by Notch: Evidence for Multiple Pathways. *J Cell Physiol* 218:84-93.
- 44 Dahlqvist C, A Blokzijl, G Chapman, A Falk, K Dannaëus, CF Ibáñez and U Lendahl. (2003). Functional Notch signaling is required for BMP4-induced inhibition of myogenic differentiation. *Development* 130:6089-6099.
- 45 Sun H, L Li, C Vercherat, NT Gulbagci, S Acharjee, J Li, TK Chung, TH Thin and R Taneja. (2007). Stra13 regulates satellite cell activation by antagonizing Notch signaling. *J Cell Biol* 177:647–657.

- 46 Quattrocelli M, D Costamagna, G Giacomazzi, J Camps and M Sampaolesi. (2014). Notch signaling regulates myogenic regenerative capacity of murine and human mesoangioblasts. *Cell Death Dis* 5:e1448.
- 47 Mourikis P and S Tajbakhsh. (2014). Distinct contextual roles for Notch signalling in skeletal muscle stem cells. *BMC Dev Biol* 14:2.
- 48 Tezuka K, M Yasuda, N Watanabe, N Morimura, K Kuroda, S Miyatani and N Hozumi. (2002). Stimulation of osteoblastic cell differentiation by Notch. *J Bone Miner Res* 17:231-239.
- 49 Engin F, Z Yao, T Yang, G Zhou, T Bertin, MM Jiang, Y Chen, L Wang, H Zheng, RE Sutton, BF Boyce and B Lee. (2008). Dimorphic effects of Notch signaling in bone homeostasis. *Nat Med* 14:299-305.
- 50 Hilton MJ, X Tu, X Wu, S Bai, H Zhao, T Kobayashi, HM Kronenberg, SL Teitelbaum, Ross FP, Kopan R and Long F. (2008). Notch signaling maintains bone marrow mesenchymal progenitors by suppressing osteoblast differentiation. *Nat Med* 14:306-314.
- 51 Cappellari O, G Cossu. (2013). Pericytes in Development and Pathology of Skeletal Muscle. *Circ Res* 113:341-347.

- 52 Birbrair A, T Zhang, ZM Wang, ML Messi, A Mintz and O Delbono. (2015). Pericytes at the intersection between tissue regeneration and pathology. Clin Sci (Lond) 128:81-93.

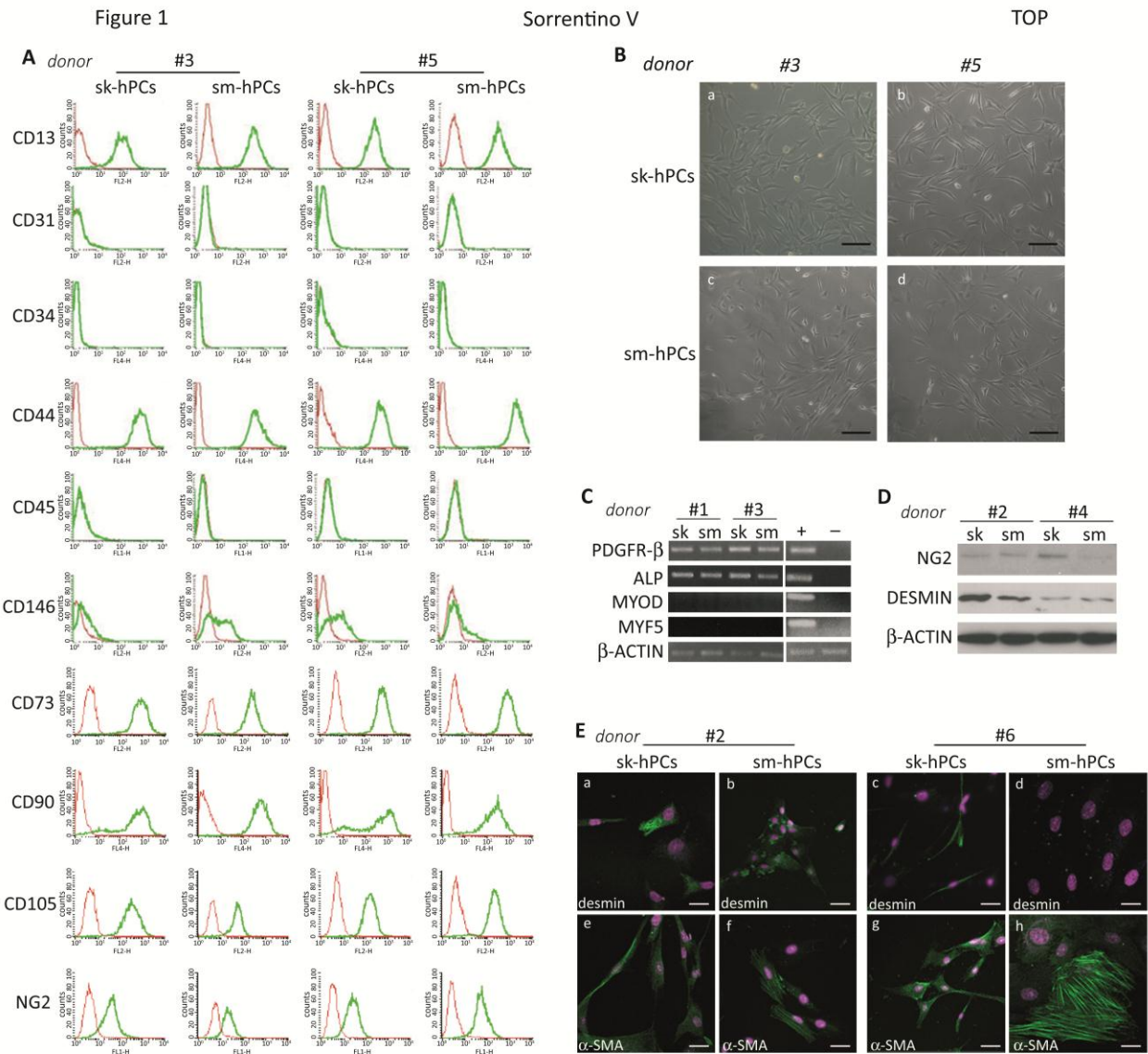


FIG. 1. Characterization of cultured pericytes from skeletal and smooth muscle tissues. (A): Flow cytometry analysis on cultured skeletal muscle-derived human pericytes (sk-hPCs) and cultured smooth muscle-derived human pericytes (sm-hPCs). Representative plots of a panel of markers (green: CD13, CD31, CD34, CD44, CD45, CD146, CD73, CD90, CD105, NG2) are shown for isogenic cell populations isolated from donors #3 and #5. Ig isotype-matched antibodies are shown in red. **(B):** Phase contrast images of isogenic sk-hPCs (a-b) and sm-hPCs

(c-d) from donors #3 and #5. Scale bars: 100 μ m. **(C):** RT-PCR analysis of the expression of PDGFR- β , ALP, MYOD and MYF5 genes in isogenic cultured pericytes from skeletal (sk) and smooth (sm) muscle of donors #1 and #3. Total RNA from human bone marrow derived mesenchymal stem cells (MSCs) and no-template samples were used as positive (+) and negative (-) controls, respectively, for PDGFR- β and ALP. Total RNA from human myoblasts and terminal differentiated osteocytes were used as positive (+) and negative (-) controls, respectively, for MYF5 and MYOD. The expression of β -actin was used as control. β -actin expression of human bone marrow MSCs and “no-template samples” are not shown. **(D):** Western blot analysis of NG2 and desmin expression in isogenic cultured pericytes from skeletal (sk) and smooth (sm) muscle of donors #2 and #4. Expression of β -actin was used as loading control. **(E):** Immunofluorescence microscopy analysis with anti-desmin (a-d) and anti- α -SMA (e-h) antibodies (both revealed in green) in sk-hPCs and sm-hPCs from donors #2 and #6. Nuclei were counterstained with TO-PRO[®]-3 Iodide. Scale bars: 20 μ m.

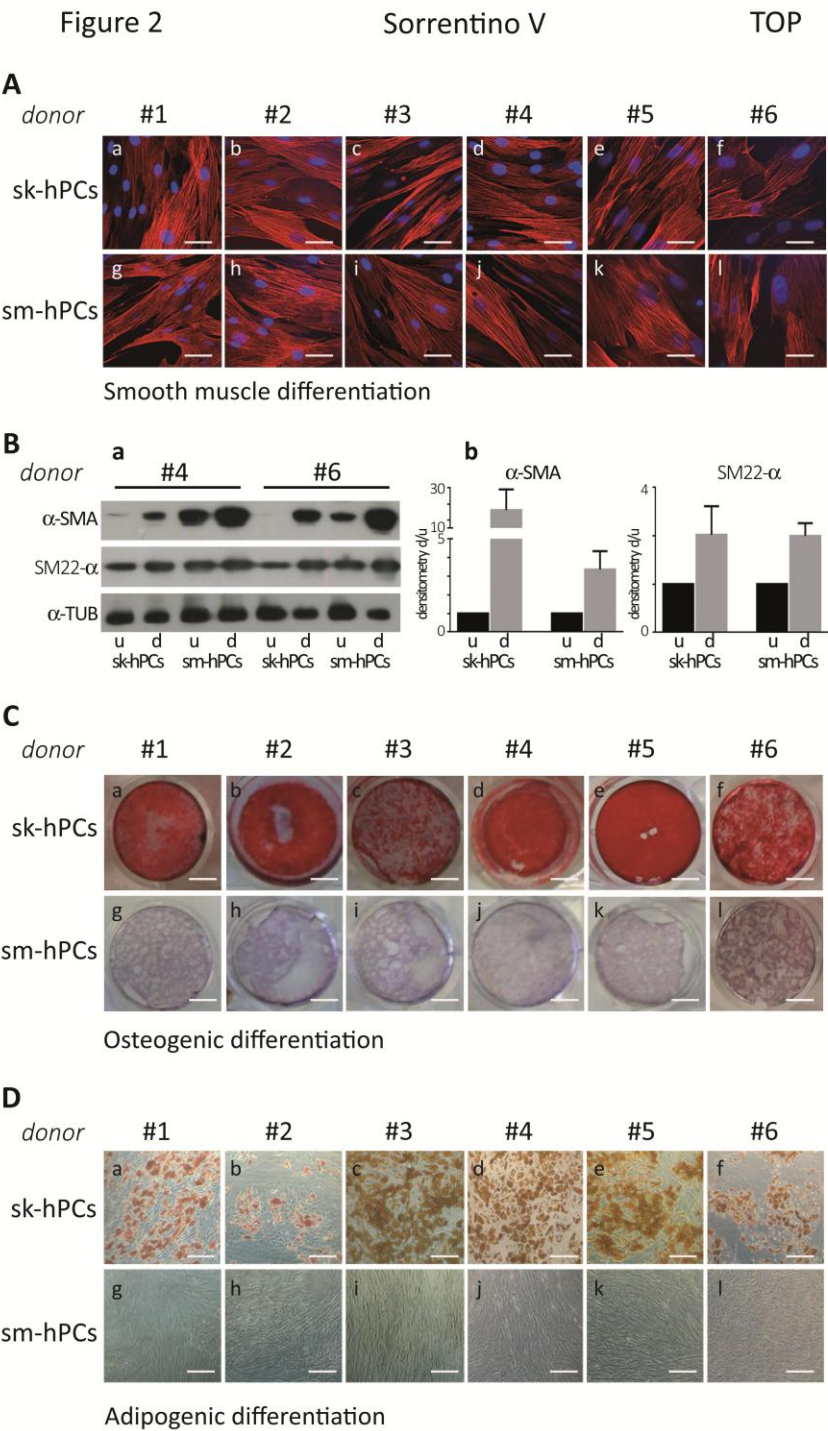


FIG. 2. Smooth muscle, osteogenic and adipogenic differentiation of sk-hPCs and sm-hPCs.

(A): Immunofluorescence analysis with anti-SM22- α (red) of isogenic sk-hPCs and sm-hPCs from all donors (#1-#6), following eight days of smooth muscle differentiation. Nuclei were counterstained with DAPI. **(B):** Western blot **(a)** and relative densitometric analysis **(b)** of the expression of α -SMA and SM22- α of isogenic sk-hPCs and sm-hPCs from donors #4 and #6 before (undifferentiated, u) and following eight days of smooth muscle differentiation (differentiated, d). α -Tubulin was used as loading control. Densitometric values relative to undifferentiated cells that are arbitrarily set as one, are reported as means + SEM (n=2). **(C):** Alizarin Red staining of calcified bone mineral matrix deposited by sk-hPCs and sm-hPCs from all donors (#1-#6). Sk-hPCs (a-f) and sm-hPCs (g-l) were stained two and four weeks after the induction of osteogenic differentiation, respectively. **(D):** Oil Red-O staining of lipid droplets in sk-hPCs (a-f) and sm-hPCs (g-l) from all donors (#1-#6). All cell populations were stained two weeks after the induction of adipogenic differentiation. For all cell populations, three experimental replicates were performed in each differentiation assay. Scale bars: 20 μ m (A), 4.35 mm (C) and 100 μ m (D).

Figure 3 Sorrentino V TOP

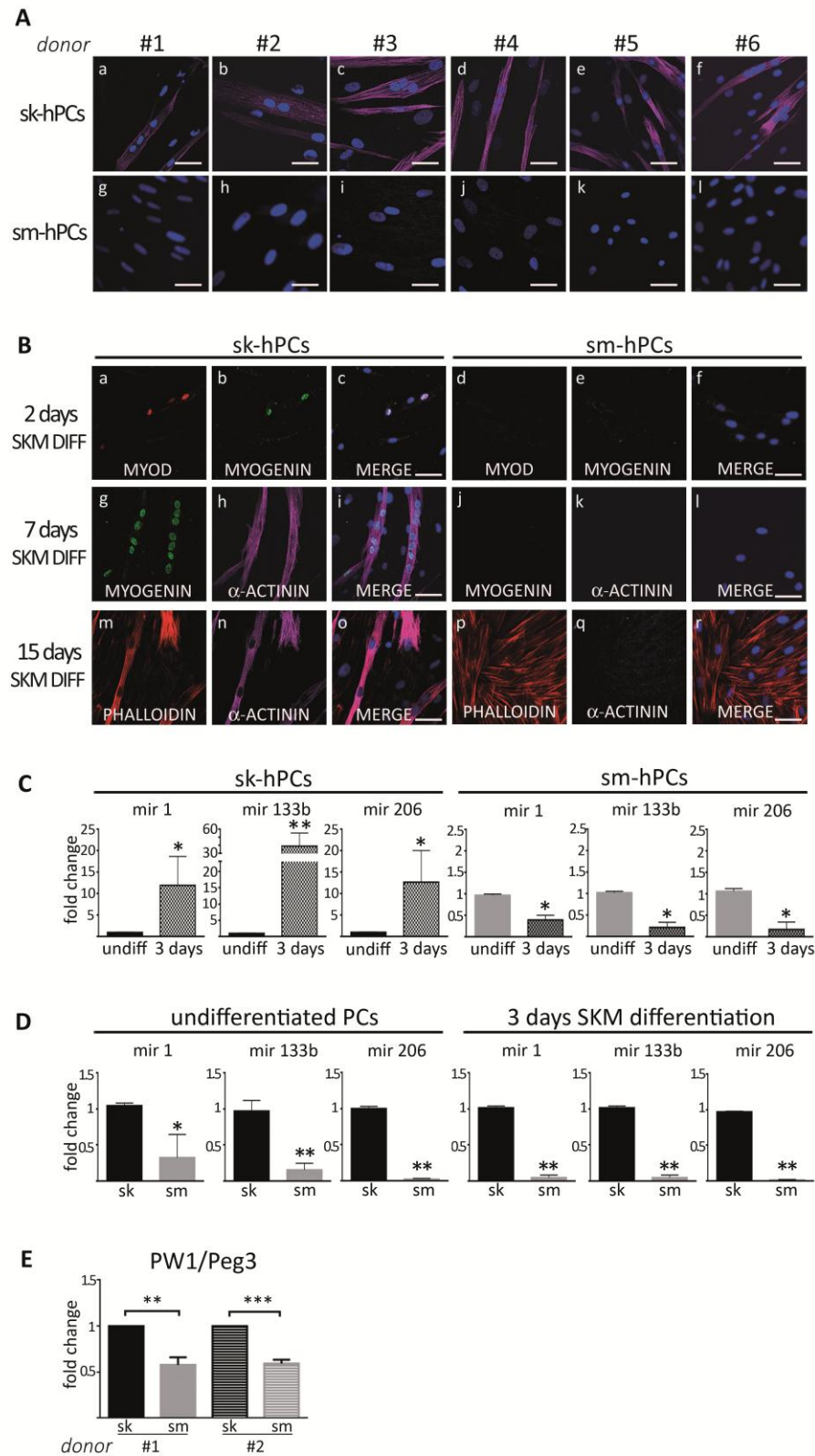


FIG. 3. Skeletal muscle differentiation of sk-hPCs and sm-hPCs. (A): Immunofluorescence analysis of α -actinin expression in isogenic sk-hPCs (a-f) and sm-hPCs (g-l) from all donors (#1-#6), ten days following induction of skeletal myogenic differentiation. Scale bars: 20 μ m. **(B):** Detailed immunofluorescence analysis of skeletal muscle differentiation of sk-hPCs (a-c, g-i, m-o) and sm-hPCs (d-f, j-l, p-r) following two (a-f), seven (g-l) and fifteen (m-r) days of differentiation. MYOD (a, c, d, f; red) and Myogenin (b, c, e, f; green) double-positive nuclei were detected after two days of differentiation only in sk-hPCs. α -Actinin (h, i, k, l; violet) positive myotubes that contain several myogenin positive nuclei (g, i, j, l) were identified at seven days of differentiation only in sk-hPCs. Fifteen days after the induction of differentiation, α -actinin positive myotubes were detected in differentiating sk-hPCs (n, o) but not in sm-hPCs (q, r). To visualize cell morphology, F-actin cytoskeleton of fifteen days differentiated cells was stained by rhodamine-conjugated phalloidin (m, o, p, r; red). All nuclei were counterstained with DAPI. For all cell populations three experimental replicates were performed in each differentiation assay. Scale bars: 20 μ m. **(C):** Relative expression analysis of mir-1, mir-133b and mir-206 in sk-hPCs and sm-hPCs following three days of skeletal muscle differentiation. The expression of each target microRNA in undifferentiated cells was used as internal reference and arbitrarily set as one. **(D):** Relative expression analysis of mir-1, mir-133b and mir-206 in undifferentiated sk-hPCs and sm-hPCs, and in differentiating sk-hPCs and sm-hPCs three days after the induction of skeletal muscle (SKM) differentiation. MyomiRs expression in sk-hPCs was used as internal reference and arbitrarily set as one in both undifferentiated and differentiating cells. **(E):** Quantitative analysis of PW1/Peg3 in undifferentiated sk-hPCs and sm-hPCs. For the analysis of relative expression, PW1/Peg3 expression in sk-hPCs was used as internal reference and arbitrarily set as one. In panels C, D and E, $2^{-\Delta\Delta Ct}$ method was used to

calculate the relative fold change of target expression. Data reported in C and D are means + SEM of six pairs of isogenic sk-hPCs and sm-hPCs. Data reported in E are the means + SD of three different experiments performed on each cell population. Statistical analysis were performed by Wilcoxon matched-pair, non-parametric T-test (C) and Mann Whitney unpaired, non-parametric T-test (D, E). Significant p -value < 0.05 ; * $p<0.05$; ** $p<0.01$; *** $p<0.001$.

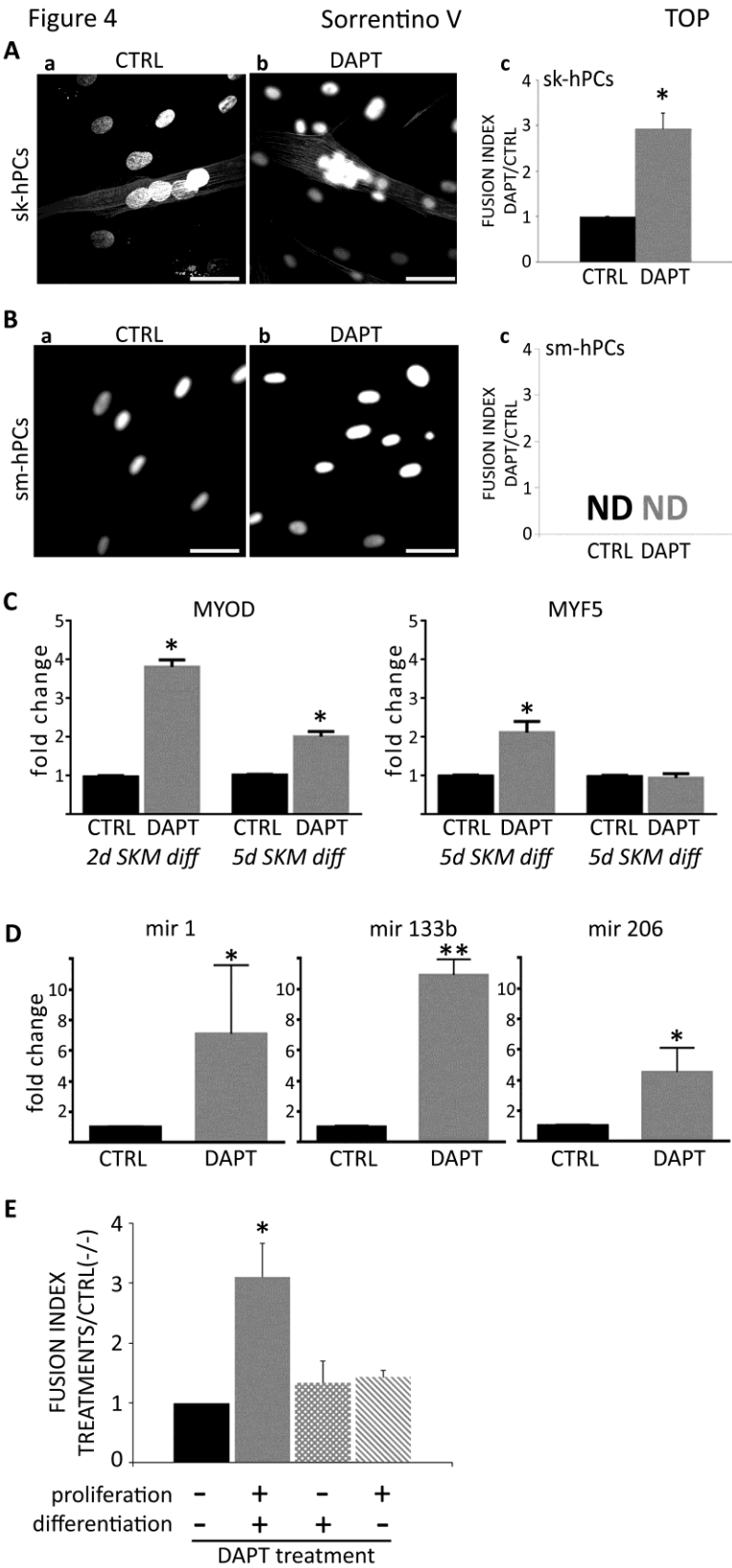


FIG. 4. Effects of Notch pathway inhibition on myogenic ability of sk-hPCs and sm-hPCs .

Representative immunofluorescence analysis of α -Actinin (violet) expression in sk-hPCs (**A**) and sm-hPCs (**B**) cultured in standard myogenic differentiation medium (CTRL, a) or in myogenic differentiation medium supplemented with N-[N-(3,5-Difluorophenacetyl)-L-alanyl]-S-phenylglycine t-butyl ester (DAPT, b), the γ -secretase inhibitor, for twelve days. Nuclei were stained with DAPI. Relative fusion index of CTRL and DAPT-treated cells are reported in the histograms in A, c and B, c. Fusion index of CTRL cells was arbitrarily set as one. Plotted data are the mean ratio + SEM of fusion index of six DAPT treated cell populations over six CTRL cell populations. Fusion index was calculated as the number of nuclei inside α -actinin positive multinucleated cells, divided by the total number of nuclei. ND = not detected. (**C**): Quantitative analysis by real-time PCR of MYOD and MYF5 expression in sk-hPCs from all donors ($n=6$), two and five days after the induction of skeletal muscle differentiation (SKM). Relative expression in CTRL and DAPT-treated cells was calculated by $2^{-\Delta\Delta C_t}$ method. MYOD and MYF5 expression in CTRL cells was arbitrarily set as one. Reported data are means + SEM (**D**): Relative expression analysis of mir-1, mir-133b and mir-206 in CTRL and DAPT-treated undifferentiated sk-hPCs from all donors ($n=6$). Relative expression between CTRL and DAPT treated cells was calculated by $2^{-\Delta\Delta C_t}$ method. MyomiR expression in CTRL cells was arbitrarily set as one. Statistical analysis were performed by Mann-Whitney unpaired, non-parametric T-test. Reported data are means + SEM (**E**): Relative myogenic differentiation efficiency of sk-hPCs cultured with (+) or without (-) DAPT administration during proliferation and/or skeletal muscle differentiation. Plotted data are the mean ratio + SEM of fusion index of three treated sk-hPCs populations over three CTRL cell populations. Fusion index of CTRL cells (-/-) was arbitrarily set as one. Significant p -value < 0.05 ; * $p < 0.05$; ** $p < 0.01$. Scale bars: 20 μ m.

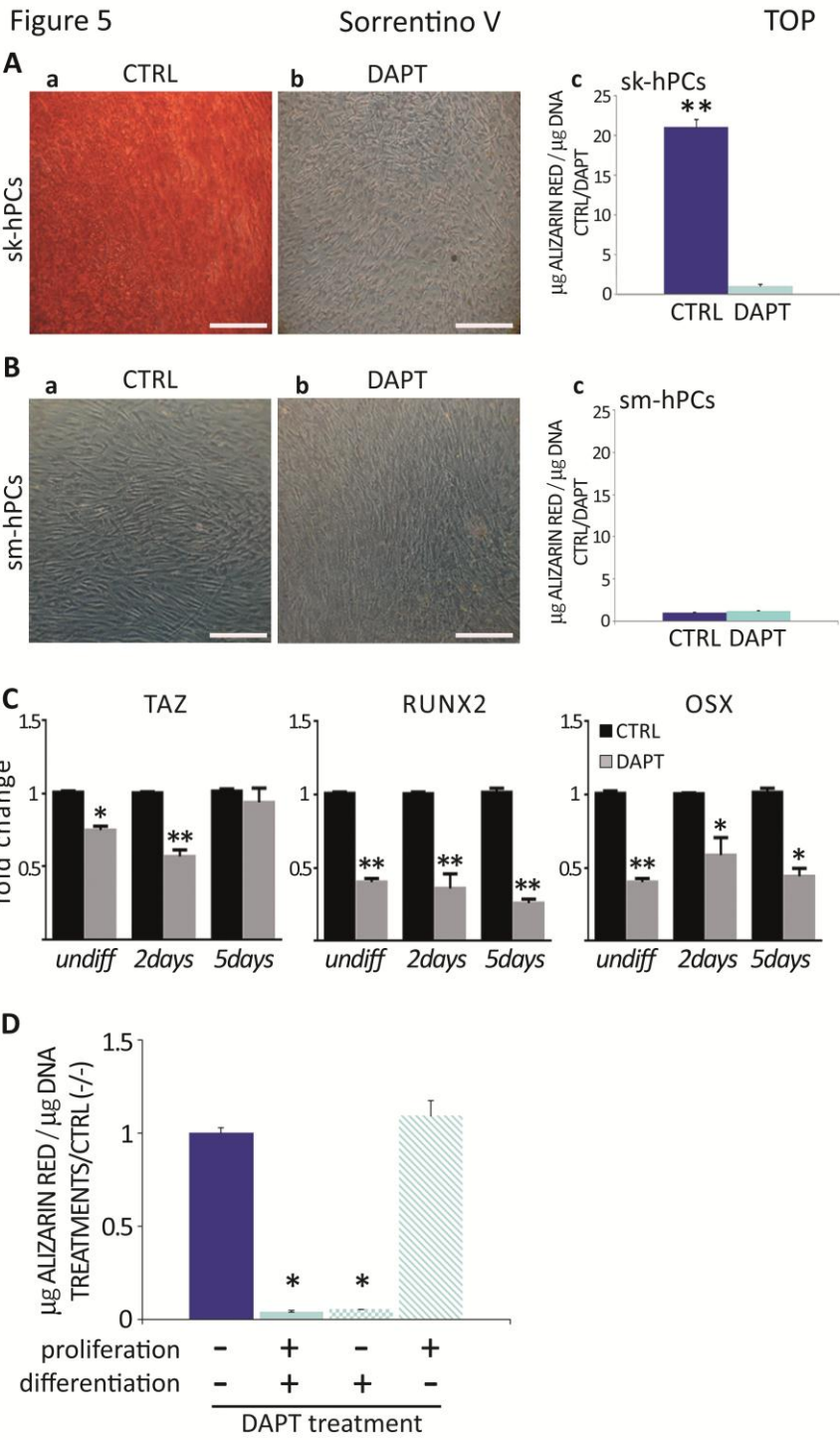


FIG. 5. Effects of Notch pathway inhibition on osteogenic ability of sk-hPCs and sm-hPCs.

Osteogenic differentiation ability of sk-hPCs (A) and sm-hPCs (B) was visualized by Alizarin

Red staining of bone mineral matrix four weeks after the induction of differentiation.

Representative micrographs of control (CTRL) and DAPT treated sk-hPCs and sm-hPCs cultured in standard osteogenic medium (CTRL, a) or in osteogenic medium supplemented with DAPT (DAPT, b). Relative quantification analysis of osteogenesis by Alizarin Red extraction in CTRL and DAPT-treated cells are reported in the histograms in A, c and B, c. The absorbance of extracted Alizarin Red was converted in μg and normalized to DNA content. Normalized Alizarin Red content of CTRL cells was arbitrarily set as one. Plotted data are the mean ratio + SEM of three different cell populations per treatment. **(C):** Quantitative analysis by real-time PCR of TAZ, RUNX2 and OSTERIX (OSX) expression of three sk-hPCs populations, before induction of differentiation and two and five days after osteogenesis induction. Relative expression between CTRL and DAPT treated cells was calculated by $2^{-\Delta\Delta\text{Ct}}$ method. TAZ, RUNX2 and OSTERIX expression in control cells was arbitrarily set as one. Reported data are means + SEM. **(D):** Relative quantification analysis of sk-hPCs cultured with (+) or without (-) DAPT administration during proliferation and/or osteogenic differentiation. Plotted data are the mean ratio + SEM of normalized Alizarin Red content of three treated sk-hPCs over three control cell populations. Significant p -value < 0.05; * p <0.05; ** p <0.01. Scale bars: 100 μm .